Applied Physics A (2018) 124:49
https://doi.org/10.1007/s00339-017-1456-6

Applied Physics A
Materials Science & Processing

Enhancement of structural and magnetic properties of M-type hexaferrite permanent magnet based on synthesis temperature

Safia Anjum[1] · Fatima Sehar[1] · Zeeshan Mustafa[2,3] · M. S. Awan[4]

Received: 10 August 2017 / Accepted: 6 December 2017 / Published online: 16 December 2017

Abstract
The main purpose of this research work is to develop the single domain magnetic particles of M-type barium hexaferrite ($BaFe_{12}O_{19}$) using oxide precursors employing conventional powder metallurgy technique. The phase formation and magnetic performance of the powders and magnets will be optimized by adjusting calcination and sintering temperatures. The synthesis of M-type barium hexaferrite was carried out in two sections. A series of four samples have been prepared by initial wet mixed powders calcined at different temperatures, i.e., 750, 850, 950 and 1050 °C. On the basis of structural analysis, the sample calcined at 950 °C has been selected and further divided into four parts to sintered them at 1100, 1150, 1200 and 1250 °C. The structural measurements depict the confirmation of M-type barium hexaferrite structure. SEM micrographs show the hexagonal-shaped grains. The abrupt decrease in coercivity for the sample sintered at 1250 °C has been seen which may be due to high sintering temperature, at which the particles have multi-domain properties.

1 Introduction

M-type hexaferrites having chemical composition $MFe_{12}O_{19,}$ where (M = Ba, Sr or Pb), are widely used in magnetic recording media, microwave devices and electromagnetic shielding fields [1, 2]. They have magnetoplumbite structure and are magnetically hard ceramic materials. Barium ferrites possess relatively high Curie temperature, coercive force and magnetic anisotropy field as well as its chemical stability and corrosion resistivity [3, 4]. Because of many unique properties, they have been a lot of interest in synthesis and characterization of different derivatives of these materials, especially in nano-scale in order to tune their great magneto-optical properties. The magnetic properties of hexaferrites such as saturation magnetization, coercivity and anisotropy field are strongly dependent on M-type phase [5, 18]. Consider pure barium hexaferrite $BaFe_{12}O_{19}$ (BaM) which has relatively high saturation magnetization, high magnetic anisotropy, high Curie temperature. These excellent magnetic properties in addition to corrosion resistance and affordable price account for bulk production of BaM [6, 17]. The challenge that interests most of the researchers is how to boost the electromagnetic character barium ferrite [7, 20]. Larger coercivity makes difficult to erase and record new data, so by optimizing the intrinsic magnetic properties, tuned electromagnetic character will be developed [8, 19]. Low saturation magnetization and coercivity H_c make the data storage and re-recordable property easy, whereas chemical inertness and longevity of the ferrite should be maintained [8–10].

Until now, barium ferrites having M-type hexagonal structure have only been used as permanent magnets and for high-density information magnetic storage [11–13]. However, a new third application of M-type hard ferrites has been discovered as a multi-ferroic material [14, 15]. These types of materials possess significant coupling between dielectric and magnetic properties. Multi-ferroic materials will widely be used in a new field of microelectronics which is known as spintronics. Spintronics uses electrically controlled magnets which require multi-ferroics with higher values of coercive field and magnetization at room temperature [16].

Multi-ferroics, which are also known as ferroelectrics, exhibit dual ferroic properties like spontaneous

✉ Safia Anjum
safia_anjum@hotmail.com

[1] Department of Physics, Lahore College for Women University, Lahore, Pakistan

[2] Department of Physics, Ningbo Institute of Materials Technology and Engineering, Chinese Academy of Sciences, Beijing, China

[3] Lahore Garrison University, Lahore, Pakistan

[4] Ibn-e-Sina, Institute of Technology, H-11/4, Islamabad, Pakistan

magnetization and specific magnetization [17, 18]. Materials having dual ferroic properties are classified by the physical origin, e.g., geometric structural transition, magnetic ordering and charge ordering [19]. The practical problems of spintronics are to design electrically controlled magnets which require multi-ferroics having higher magnetization and coercive force at room temperature. $BiFeO_3$ is the most extensively used multi-ferroic material [20]. It has low magnetic properties at higher temperature, which is the major disadvantage of this material [21]. Because of this, hexagonal ferrite-based multi-ferroics are the most promising candidates at room temperature.

$BaFe_{12}O_{19}$ provides a wide range of potential applications such as novel memory media, multiple-state memory elements, new functional sensors and transducers [22]. The $BaFe_{12}O_{19}$ having hexagonal magnetoplumbite structure was determined by Adelskold [23]. The unit cell contains two formula units, having 38 oxygen ions, 24 iron ions and 2 barium ions. The ions of iron occupy nine sixfold octahedral sites, one fivefold trigonal sites and two fourfold tetrahedral sites. Barium ions occupy 2d sites [24]. Because barium ferrites have large magneto-crystalline anisotropy, large magnetization, high curie temperature and excellent chemical stability so their anisotropy energy constant exceeds the values of garnet ferrites by a 100 times more. Materials which possess both properties of ferro-elctricity and ferromagnetism are rare. They mostly provide weak ferromagnetism. Therefore, large ferroelectricity and ferromagnetism provide a new direction for potential multi-ferroic candidate. $BaFe_{12}O_{19}$ is one of these candidates having hexagonal crystal structure [25]. The magneto-electric characteristics are more advanced in $BaFe_{12}O_{19}$ than $BiFeO_3$ multi-ferroic material. By applying the external electric field, the magnetization will be increases up to 9%. This suggests a big practical potential application of M-type hexaferrite ceramics as devices with strong magneto-electric coupling [26]. The combination of high coercive force with rather high residual induction allows to receive permanent magnets with satisfactory specific magnetic energy. Their low conductivity allows to apply hexaferrite magnets in the presence of high frequency magnetic fields [27].

Several synthesis methods have been developed to obtain low production cost of barium ferrite particles [28, 29]. Among the available chemical processes, sol gel method and solid-state reaction method, the solid state reaction method is known to be a simple and cost effective way to prepare barium ferrites with low coercive fields [2, 30–33]. Ferromagnetic nature of BaM originates from its $24F^{3+}$ ions in a unit cell, and these ferric ions exist in three crystallographically different lattices: tetrahedral ($2f_1$), trigonal (2b) and octahedral (12k, 2a and $4f_2$). 16Fe have their spin direction parallel to the crystallographic *c* axis forming the majority ↑ (12k, 2a and 2b) while 8Fe resides in the reverse direction and thus minority sub lattices ↓ ($4f_1$ and $4f_2$) [34, 35].

The aim of this research work is to see the effect of different synthesis parameters on nano-structured M-type $BaFe_{12}O_{19}$ powder in order to tune the magnetic properties.

2 Experimental setup

2.1 Sample preparation

M-type hexagonal barium ferrite ($BaFe_{12}O_{19}$) powder is synthesized using raw materials of iron oxide (Fe_2O_3) and barium carbonate ($BaCO_3$) using powder metallurgy route.

The experimental setup was carried out in two steps as shown in Fig. 1. First step is the confirmation of phase and the second one is optimization of sintering temperature to produce good magnetic performance.

The first step of the experiment is stoichiometric amounts of barium carbonate ($BaCO_3$) and iron oxide (Fe_2O_3) are taken and mixed in a ball mill using wet mill process. For wet milling, some amount of organic fluid acetone is added to get the fine homogeneous mixture. The milling process has been carried out for 1 h. The powder to ball mass ratio is taken as 1:8. After grinding, mixture was taken out into a beaker and then placed in an oven at 60 °C for 1 h. The grinding mixture is divided into four equal parts and heat treated in an electric furnace in the temperature range (750, 850, 950 and 1050 °C) to obtain the required crystallographic phase under specific conditions of time and temperature. The $BaFe_{12}O_{19}$ phase is confirmed at 950 °C, after the confirmation of the phase all of the remaining powder was annealed at 950 °C.

Second step of this experiment is the optimization of sintering temperatures. The basic purpose of this step is to prepare cylindrical magnets having enhanced magnetic properties. In this step first of all, the phase confirmed powder is further divided equally into four parts and made four pellets and then again heat treated at different sintering temperatures from 1100, 1150, 1200 and 1250 °C. Then, the final cylindrical magnets are ready to use in different characterizations. Figure 1 shows the flow chart for the preparation of Barium hexa-ferrites.

3 Results and discussion

3.1 DSC/TGA analysis

The M-type barium hexaferrites have been prepared using two starting materials Fe_2O_3 and $BaCO_3$. The DSC of barium carbonate has been carried out to check its thermal behavior and phase transition temperature. The study

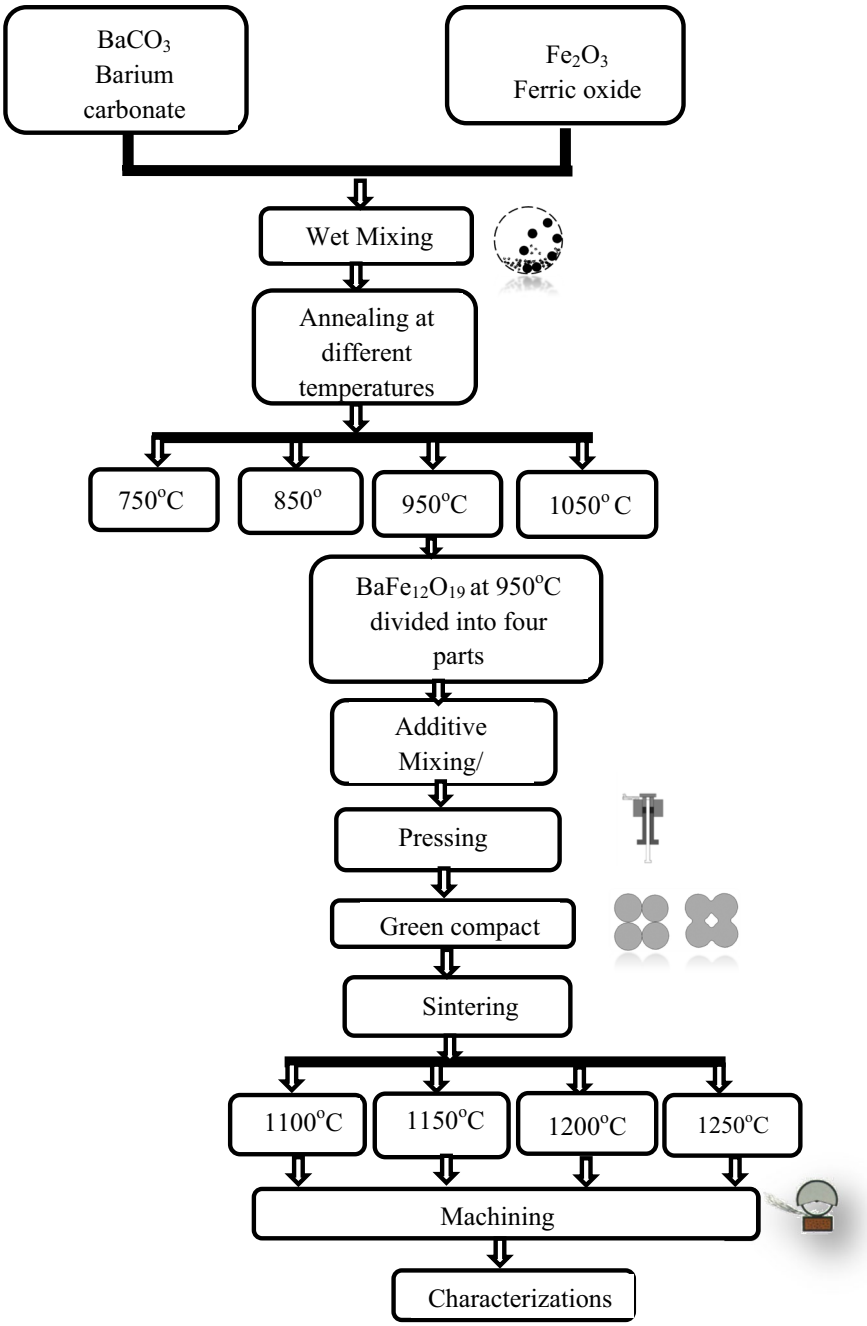

Fig. 1 Flow chart for the preparation of $BaFe_{12}O_{19}$

of phase transition temperature is necessary because it is the pre-investigation method to find the optimum temperature for the synthesis of the single domain particles. The $BaCO_3$ powder actually shows three crystallographic phases: these are rhombohedral, β-hexagonal and α-cubic. The two endothermic peaks at temperature 812 °C (1085 K) and 981 °C (2235 K) have been seen through DSC micrograph as shown in Fig. 2. These peaks might be correspond to the phase transition from γ–β and then β–α. The $BaCO_3$ thermally decomposes and, as a result, gives metal oxide and carbon dioxide (CO_2) gas. Thermal decomposition is the process in which compounds are splits by heating. Barium carbonate is thermally stable and reduced to $BaCO_2$ which is unstable [36, 37]:

$$BaCo_3 + CO \rightarrow BaCO_2 + CO_2.$$

Then, $BaCO_2$ further breaks down and gives BaO plus CO_2. The DSC micrograph exhibits that $BaCO_3$ first reduces to unstable $BaCO_2$ at 812 °C and then further decomposes to BaO at 981 °C, so latter is the temperature

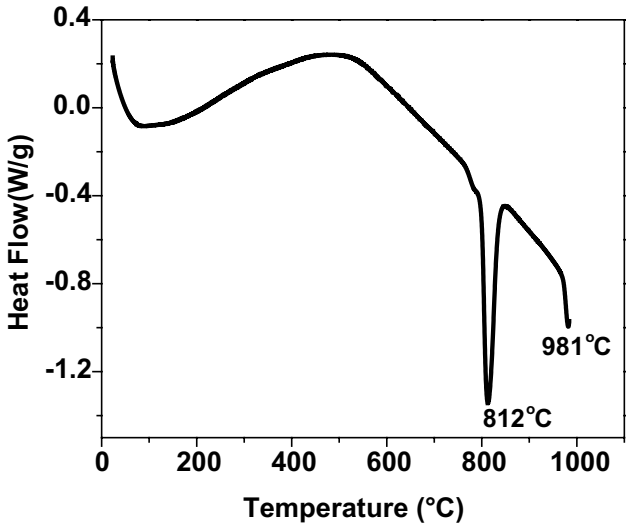

Fig. 2 DSC micrograph of $BaCO_3$

where M-type barium hexaferrite phase first starts to appear, which is also further confirmed by XRD.

The variation of weight loss (%) of $BaCO_3$ with temperature is shown in Fig. 3. There is initially a sluggish trend in mass drop with temperature but at above 871 °C the sudden change in mass is observed which might be due to the decomposition of $BaCO_3$ into BaO with the release of CO_2 gas.

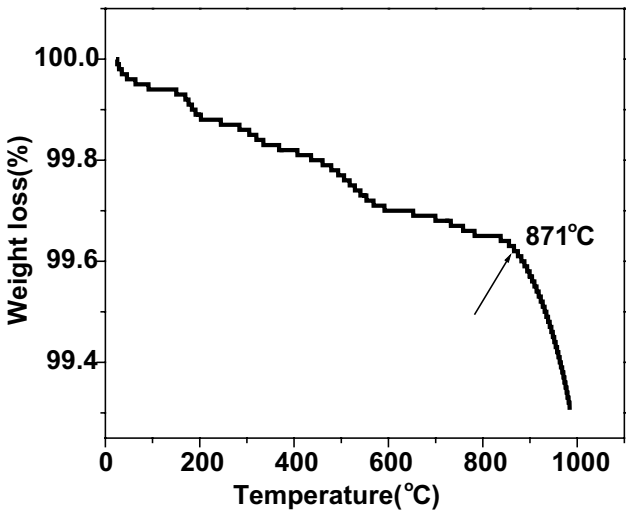

Fig. 3 TGA micrograph of $BaCO_3$

3.2 Section I

3.2.1 XRD analysis

The structural analysis of M-type barium hexaferrites annealed at different temperatures, i.e., 750, 850C, 950 and 1050 °C has been carried out using XRD machine. The comparative XRD micrograph is shown in Fig. 4.

It is observed from the comparative XRD micrograph that there is a drastic change in structure and peak intensities of the sample as the annealing temperature increases. The as-milled mixture exhibits the separate peaks of $BaCO_3$ and Fe_2O_3 mentioned on the graph. The sample sintered at 750 °C shows the amorphous-like structure and exhibits the peaks of barium mono-ferrite ($BaFe_2O_4$), barium carbonate ($BaCO_3$) and iron oxide (Fe_2O_3). These are the secondary phases which are confirmed by standard JCPD cards of $BaFe_2O_4$ (70-2468), $BaCO_3$ (045-1471) and Fe_2O_3 (01-1053). It might be that this temperature may not be suitable for the formation of M-type barium hexaferrite. The sample annealed at 850 °C exhibits the first appearance of M-type barium hexaferrite phase but some secondary phases of $BaFe_2O_4$ (70-2468), $BaCO_3$ (045-1471) and Fe_2O_3 (01-1053) are also still observed. At 950 and 1050 °C, all the secondary phases disappear and single M-type barium hexaferrite phase has been obtained which is not in accordance with the previous literature [38]. It is concluded that as the annealing temperature increases, secondary phases of Fe_2O_3, $BaCO_3$ and $BaFe_2O_4$ (barium ferrite mono phase) gradually decrease leading to the formation of single phase M-type barium hexaferrite having the composition $BaFe_{12}O_{19}$. The XRD micrographs confirmed the structure of M-type barium hexaferrite, annealed at 950 and 1050 °C. The lattice constants are calculated using the given formula [39];

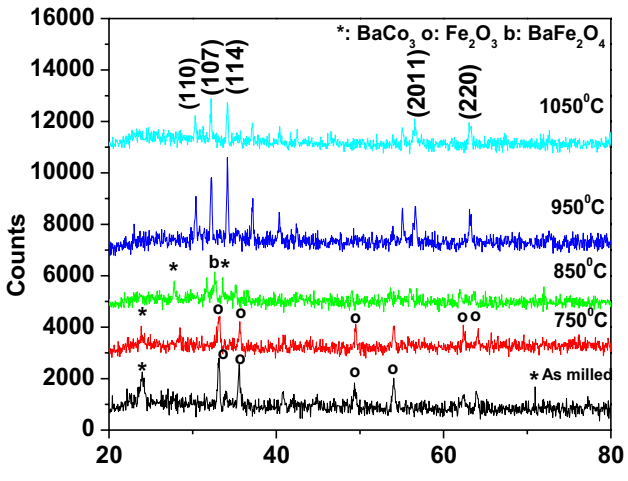

Fig. 4 Comparative XRD pattern of $BaFe_{12}O_{19}$ annealed at different temperatures

$$\frac{1}{d_{hkl}^2} = \frac{4}{3}\left(\frac{h^2 + hk + k^2}{a^2}\right) + \frac{l^2}{c^2}. \quad (1)$$

The lattice constants a and c along with the unit cell volume of these samples are listed in Table 1. The diamond software is used for the 3-D visualization of structure. The XRD structure is visualized with the help of diamond structure in which Wyckoff sites and x, y, z values of each element present in the composition are needed.

3.2.2 Diamond structure

The 3-D structural view of M-type barium hexaferrites annealed at 950 and 1050 °C is shown in Fig. 5a, b, respectively. The XRD study of M-type barium hexaferrites annealed at 950 and 1050 °C shows that the peak intensities are well indexed with the hexagonal cell having space group P 63/m m c (no. 194). There are 24 Fe^{+3} ions in five symmetry sites in which three are in octahedral site, two in tetrahedral site and one in bipyramidal site. The wykoff sites and x, y, z values for all the elements used in M-type barium hexaferrites composition are listed in Table 2.

The cell volumes of M-type barium hexaferrites annealed at 950 and 1050 °C are calculated using the formula given below. These cell volume values are then further confirmed with the help of diamond software [29, 30].

$$V = a^2 c\sqrt{3}/2. \quad (2)$$

Table 1 XRD data for barium ferrite

Annealing temperature T (°C)	Lattice parameter a (A^0)	Lattice parameter c (A^0)	Volume V (A^{03})
950	5.8866	23.1371	694.33
1050	5.8793	23.1986	694.45

Table 2 Atomic coordinates of $BaFe_{12}O_{19}$

Atom	Oxidation no.	Wyckoff site	x	y	z
O	−2	12k	0.5	1.00	0.15
O	−2	12k	0.16	0.33	0.05
O	−2	6h	0.5	1.00	0.25
O	−2	4f	0.33	0.66	−0.05
O	−2	4e	0	0	0.15
Fe	+3	12k	0.16	0.33	−0.10
Fe	+3	4f	0.33	0.66	0.02
Fe	+3	2b	0	0	0.25
Fe	+3	2a	0	0	0
Ba	+2	2d	0.66	0.33	0.25

The wyckoff sites and x, y, z values for all the elements present in $BaFe_{12}O_{19}$ composition are listed in Table 2.

These micrographs show that there is a slight difference in both structures because of the small variation in lattice parameters of the samples annealed at 950 and 1050 °C. It is observed from Table 1 that lattice parameter a decreases whereas c increases; hence as a result the cell volume of the sample annealed at 1050 °C is slightly greater than that of 950 °C.

3.2.3 SEM analysis

The SEM micrographs of M-type barium hexaferrites annealed at different temperatures, i.e., 750, 850, 950 and 1050 °C, are shown in Fig. 6a–d, respectively.

It is observed from the Fig. 6a for the sample annealed at 750 °C that there is an amorphous-like structure with the very small particles of the order of few nanometers, with no definite shape distributed in a random fashion. The second sample annealed at 850 °C is shown in Fig. 6b, it is observed that the grain size has been increased due to more diffusion at comparatively high temperature. The

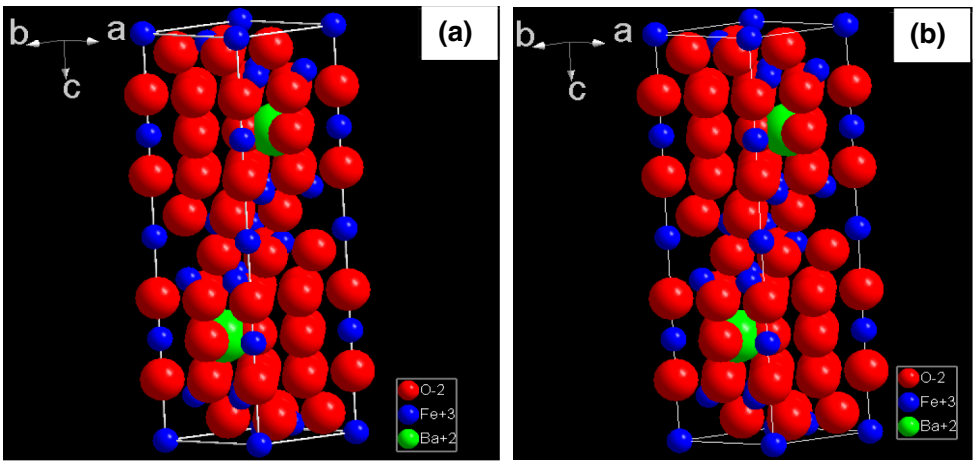

Fig. 5 3-D structure of $BaFe_{12}O_{19}$ annealed at **a** 950 °C and **b** 1050 °C

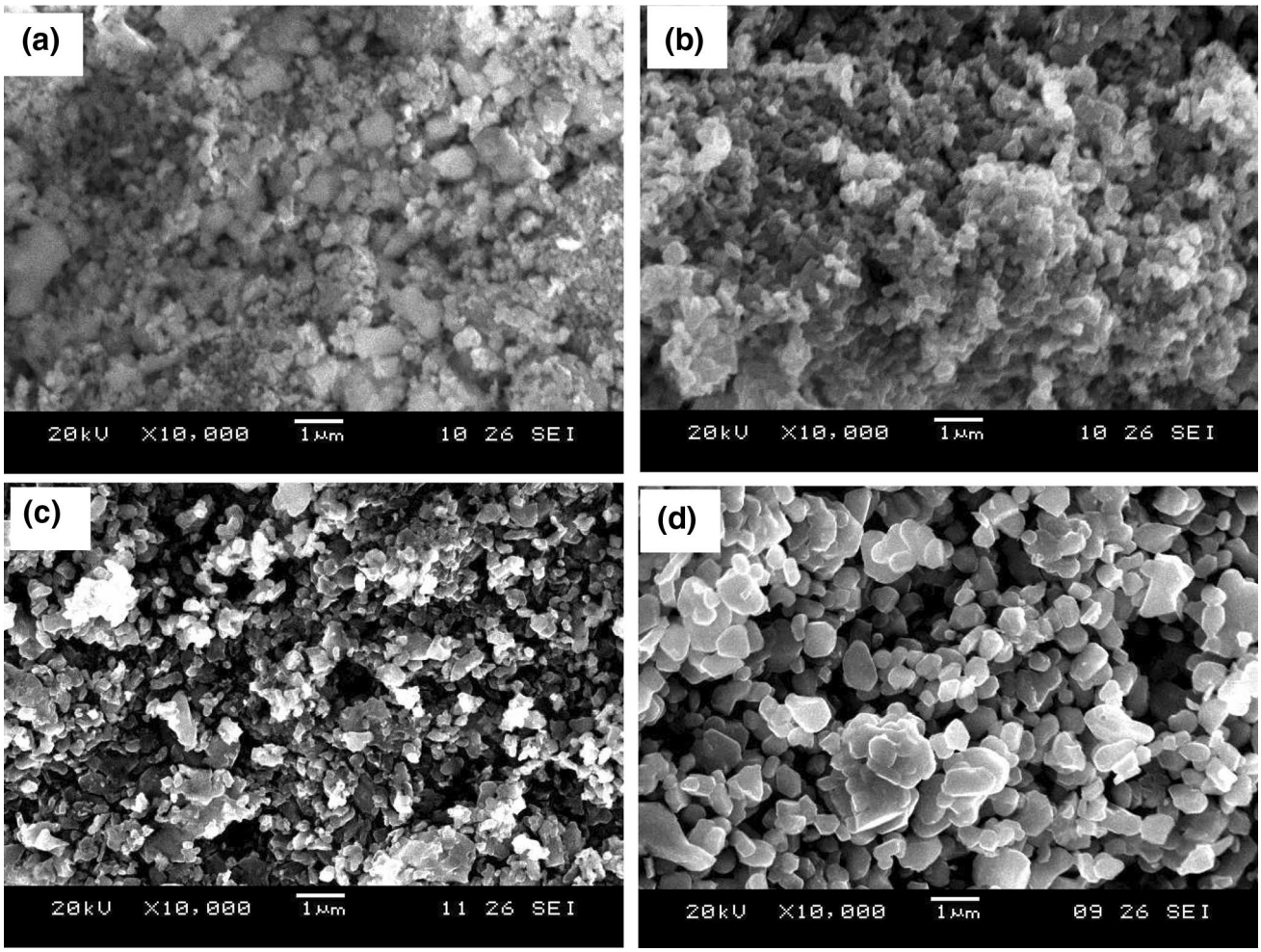

Fig. 6 SEM micrographs of $BaFe_{12}O_{19}$ annealed at **a** 750 °C, **b** 850 °C, **c** 950 °C and **d** 1050 °C

well-defined spherical and elongated shaped grains have been seen in the SEM micrograph of the M-type barium ferrite annealed at 950 °C as shown in Fig. 6c. The development of definite shape and well-defined boundary of these partial hexaferrite grains might be due to the proper annealing of temperature. This is also evident from XRD micrographs that barium hexagonal ferrite phase first appears at 950 °C. The small hexagonal-shaped grains with definite arrangement have been observed in Fig. 6d for the samples annealed at 1050 °C. The increment in annealing temperature results in pure phase of M-type barium hexaferrite with better demonstration of grain shape and boundary. After the formation of single phase M-type barium ferrite at 950 °C, the sample is further distributed into four equal parts and then optimizes the sintering temperature ranges from 1100, 1150, 1200 and 1250 °C. The prepared samples are then characterized through XRD, FTIR, SEM and DC-magnetometer. These are explained further in detail in section II below:

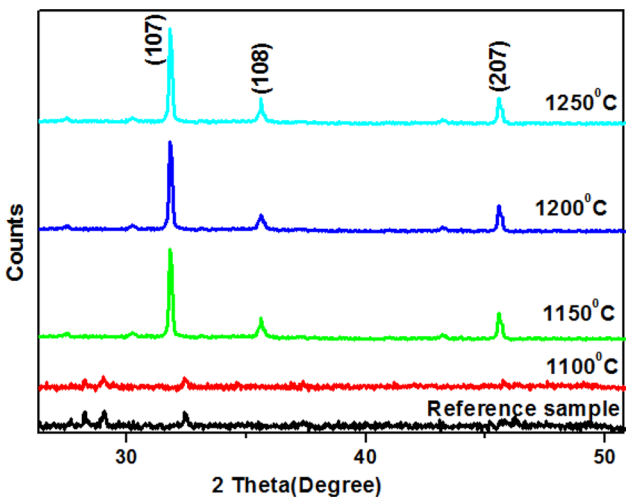

Fig. 7 Comparative XRD micrographs of $BaFe_{12}O_{19}$ sintered at different temperature

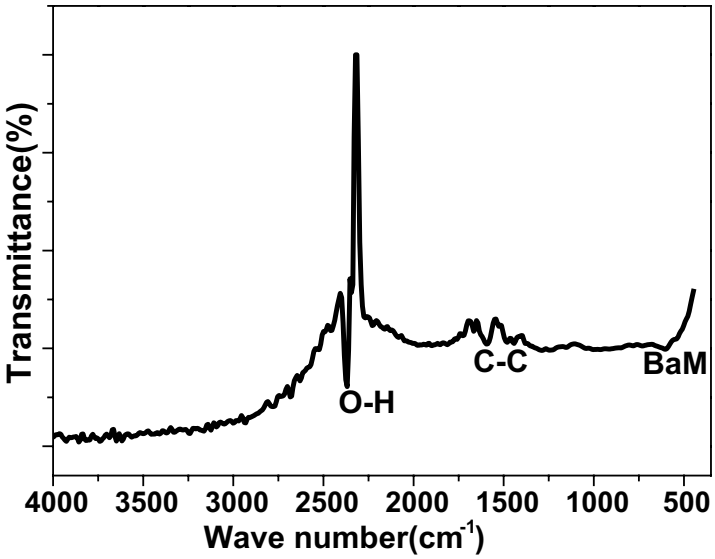

Fig. 8 FTIR micrograph of $BaFe_{12}O_{19}$ sintered at 1250 °C

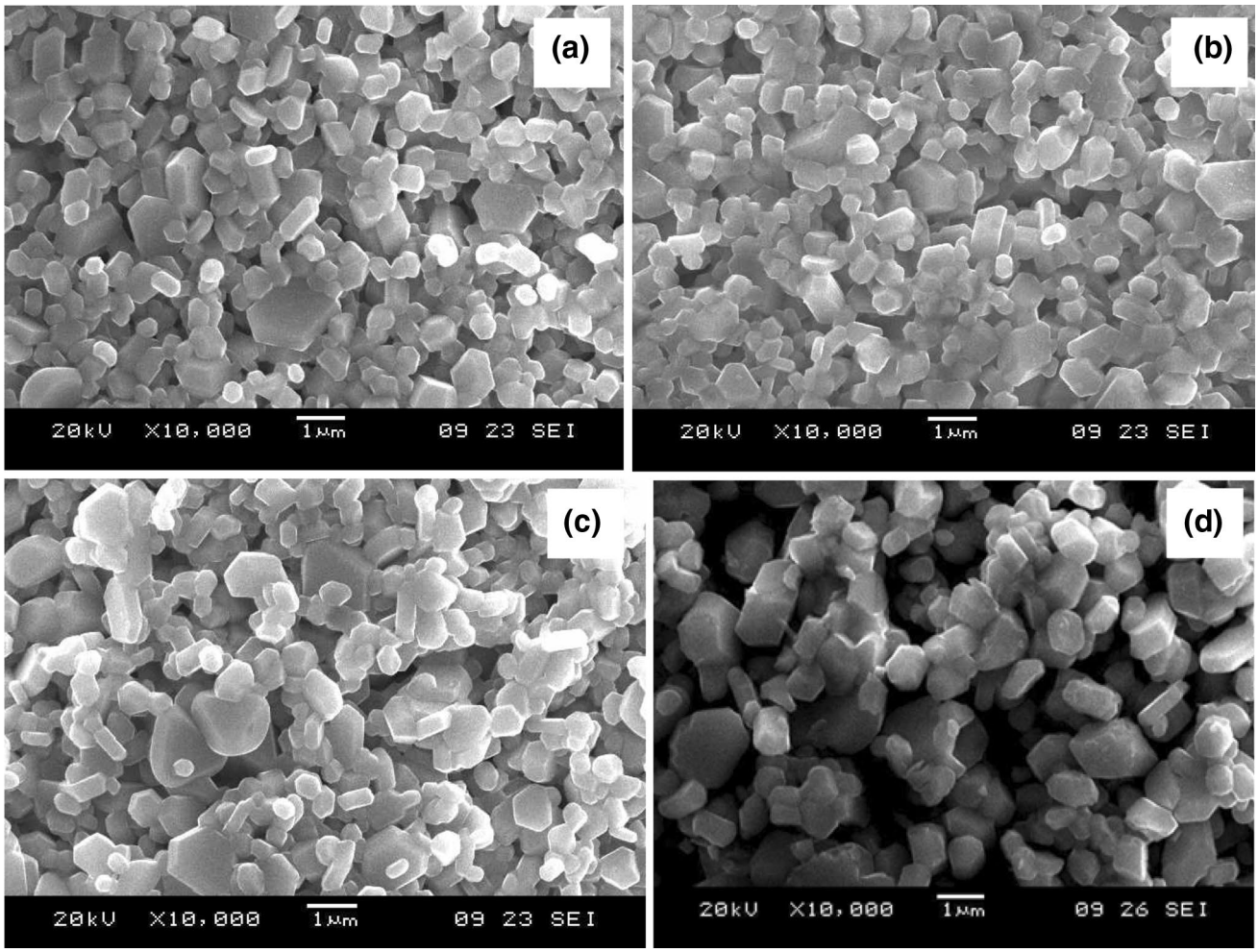

Fig. 9 SEM micrographs of $BaFe_{12}O_{19}$ sintered at **a** 1100 °C, **b** 1150 °C, **c** 1200 °C and **d** 1250 °C

3.3 Section II

3.3.1 XRD analysis

The XRD micrographs of $BaFe_{12}O_{19}$ sintered at 1100, 1150, 1200 and 1250 °C are shown in Fig. 7. These XRD micrographs exhibit that as the sintering temperature increases, the grain size increases. At high sintering temperature, the thermal energy of the particles increases significantly, which force to diffuse the particles to make a bigger grain. It may also be due to the alignment of more planes in their specific directions and, as a result, the intensity of peaks becomes sharper.

3.3.2 FTIR analysis

The structural verification of M-type barium hexaferrite sintered at 1250 °C is again carried out through FTIR. The IR spectra for the M-type barium hexaferrites have been recorded between 500 and 4000 cm^{-1} as shown in Fig. 8. The typical metal–oxide vibration band verifies the hexagonal structure which is generally in the range 450–600 cm^{-1}. The band at 592 cm^{-1} in Fig. 8 suggests the intrinsic stretching vibrations of metal (Fe ← – → O) which confirms the hexagonal structure BaM. It verifies that the precursors are fully decomposed and form barium hexagonal ferrite (BaM). It is in good agreement with the reported literature [40]. The absorption band located at

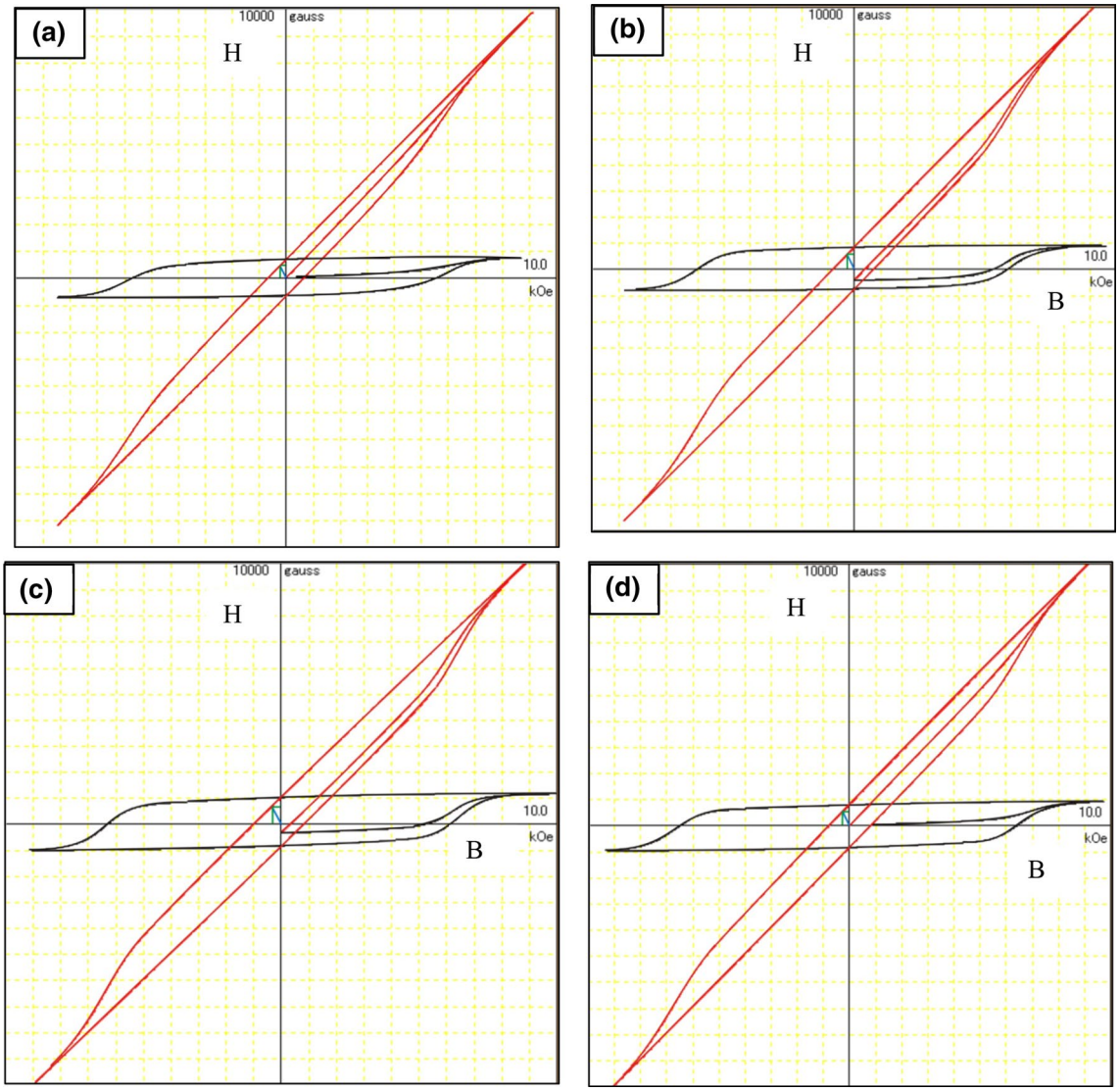

Fig. 10 Comparative DC magnetometer micrographs of $BaFe_{12}O_{19}$ sintered at **a** 1100, **b** 1150, **c** 1200 and **d** 1250 °C

1661 cm^{-1} is of C=C. This bond might be due to CO_2 in air and most probably due to the burning of gasses in the furnace. The band located at 2371 cm^{-1} may be attributed to the symmetric vibration of –OH groups. It may be due to the presence of KBr which is used for the preparation of FTIR pellet.

3.3.3 SEM analysis

The SEM micrographs of M-type barium hexaferrites sintered at different temperatures, i.e., 1100, 1150, 1200 and 1250 °C, are shown in Fig. 9a–d, respectively.

It is observed from SEM micrographs for the samples sintered at 1100, 1150 and 1200 °C that it exhibits a lot of small hexagonal-shaped particles with definite grain boundaries, having grain size 625–375 nm. The remarkable feature is observed in the SEM micrograph for the sample sintered at 1250 °C that shows larger grains of about 950 nm with plate-like structure. It is concluded that at 1250 °C sintering temperature or above this temperature, the grain size noticeably increases which is also evident from XRD analysis.

3.3.4 Magnetic properties

DC-magnetometer is used to determine magnetic properties of the sample. The hysteresis loops of M-type barium hexaferrites sintered at different temperatures such as 1100, 1150, 1200 and 1250 °C are shown in Fig. 10a–d, respectively. The parameters extracted from hysteresis loops are tabulated in Table 3. These micrographs show both MH (black) and BH (red) curves of M-type barium hexaferrites. These curves depict the broad MH loop, which is the confirmation of the hard hexagonal barium ferrite. It is observed that as the sintering temperature increases up to 1150 °C, the coercivity also increases, which might be due to the single domain particles. In single domain particles, the coercivity has remarkable relation with grain size [41–46]. But as the sintering temperature reaches 1250 °C, the coercivity decreases slightly due to the multi-domain properties of particles. The relationship between the coercivity and grain size as a function of sintering temperature is shown in Fig. 11 which is also in good agreement with the literature [47]. It is also noticed that the energy density of M-type hexaferrites increases at elevated temperature which is also the confirmation of the formation of stronger magnets as compared to the magnet at low sintering temperature.

Table 3 Magnetic properties of M-type barium hexaferrite sintered at 1100, 1150, 1200 and 1250 °C

Temperature (°C)	Br (Oe) × 10^2	iH_c (KOe)	BH_{max} (MOe) × 10^{-1}	Grain size (nm)
1100	7.22	5.751	1.262	625
1150	8.45	6.024	1.775	425
1200	8.02	6.490	1.558	375
1250	1.03	6.310	2.556	950

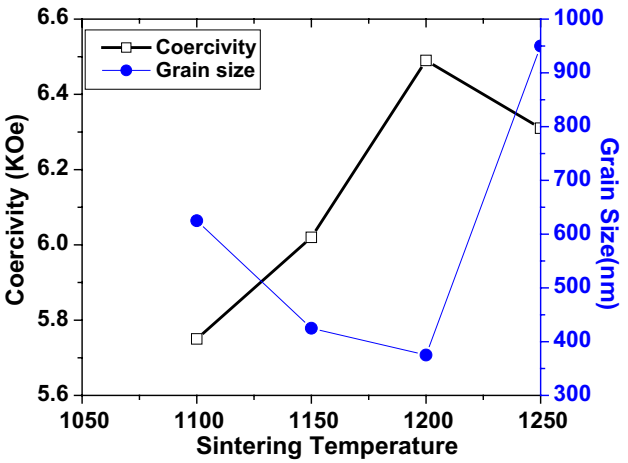

Fig. 11 Showing the relation between coercivity and grain size with different sintering temperatures

4 Conclusion

A series of M-type barium hexaferrites have been synthesized at different annealing temperatures from 750, 850, 950 and 1050 °C in section I and then again sintered them at 1100, 1150, 1200 and 1250 °C to study the effect of temperature on structural and magnetic properties. The structural analysis revealed that as the sintering temperature goes towards the elevated temperature the intensity of the peaks becomes more intense and sharp; as a result, the perfect single phase hexagonal structure is achieved. FTIR analysis confirmed the single phase of M-type barium hexaferrite with the major band at 592 cm^{-1}, which might be due to the stretching vibrations of metal–oxide bond. The magnetic properties confirm the formation of stronger magnets due to the high energy density and coercivity. So we may suggest that these M-type hexaferrites are the potential candidate used as a core in transformer and for storage devices.

References

1. N. Shams, X. Liu, M. Matsumoto, A. Morisako, Manipulation of crystal orientation and microstructure of barium ferrite thin film. J. Magn. Magn. Mater. **290–291**, 138–140 (2005)
2. O. Carp, R. Barjega, E. Segal, M. Brezeanu, Nonconventional methods for obtaining hexaferrites. Thermochim. Acta **318**, 57–62 (1998)

3. J. Ding, W.F. Miao, P.G. McCormick, R. Street, High coercivity ferrite magnets prepared by mechanical alloying. J. Alloy. Compd. **281**, 32–36 (1998)
4. A. Mali, A. Ataie, Structural characterization of nano crystalline $BaFe_{12}O_{19}$ powders synthesized by sol–gel combustion route. Scr. Mater. **53**, 1065–1075 (2005)
5. L. Lechevallier, J.M. Le Breton, J.F. Wang, I.R. Harris, Effects of Gd substitution on the structural and magnetic properties of strontium hexaferrites. J. Magn. Magn. Mater. **269**, 192 (2004)
6. R.C. Pullar, Hexagonal ferrites: a review of the synthesis, properties and applications of hexaferrite ceramics. Prog. Mater. Sci **57**, 1191–1334 (2012)
7. I.A. Auwal, A. Baykal, H. Güngüneş, S.E. Shirsath, Structural investigation and hyperfine interactions of $BaBi_xLa_xFe_{12-2x}O_{19}$ ($0.0 \leq x \leq 0.5$) hexaferrites. Ceram. Int. **42**, 3380–3388 (2016)
8. R. Gerber, R. Atkinson, Z. Simsa, Magnetism and magneto-optics of hexaferrite layers. J. Magn. Magn. Mater. **175**, 79–89 (1997)
9. E.W. Gorter, Saturation magnetization and crystal chemistry of ferromagnetic oxides. Philos. Res. Rep **9**, 295–320 (1954)
10. I.A. Baykala, S. Auwalb, H. Gunerc, Sozerid, Magnetic and optical properties of Zn^{2+} ion substituted barium hexaferrites. J. Magn. Magn. Mater. **430**, 29–35 (2017)
11. S.V. Trukhanov, A.V. Trukhanov, V.G. Kostishin, L.V. Panina, I.S. Kazakevich, V.A. Turchenko, V.V. Kochervinskiie, Coexistence of spontaneous polarization and magnetization in substituted M-type hexaferrites $BaFe_{12-x}Al_xO_{19}$ ($x \leq 1.2$) at room temperature. JETP Lett. **103**(2), 100–105 (2016) (Condensed Matter, ISSN 0021-3640)
12. E. Richter, T.J.E. Miller, T.W. Neumann, T.L. Hudson, Overview of research evolution in the field of line start permanent magnet synchronous motors. IEEE Trans. Ind. Appl. **21**, 644 (1985)
13. G. Tan, X. Chen, Structure and multi ferroic properties of barium hexa-ferrite ceramics. J. Magn. Magn. Mater. **327**, 87–90 (2013)
14. Y. Tokunaga, Y. Kaneko, D. Okuyama, S. Ishiwata, T. Arima, S. Wakimoto, K. Kakurai, Y. Taguchi, Y. Tokura, Multiferroic M-type hexaferrites with a room-temperature conical state and magnetically controllable spin helicity. Phys. Rev. Lett. **105**, 257201 (2010)
15. S.V. Trukhanov, A.V. Trukhanov, V.G. Kostishyn, L.V. Panina, An.V. Trukhanov, V.A. Turchenko, D.I. Tishkevich, E.L. Trukhanova, O.S. Yakovenkog, L. Yu. Matzuig, Investigation into the structural features and microwave absorption of doped barium hexa-ferrites. Dalton Trans. **46**, 9010–9021 (2017),
16. A.S. Logginov, G.A. Meshkov, A.V. Nikolaev, A.P. Pyatakov, Magnetoelectric control of domain walls in a ferrite garnet film. JETP Lett. **86**(2), 115–118 (2007)
17. A.V. Trukhanov, S.V. Trukhanov, L.V. Panina, V.G. Kostishyn, D.N. Chitanov, I.S. Kazakevich, A.V. Trukhanov, V.A. Turchenko, M.M. Salem, Strong correlation between magnetic and electrical subsystems in diamagnetically substituted hexaferrites ceramics. Ceram. Int. **43**, 5635–5641 (2017)
18. P. Niemiec, D. Bochenek, A. Chrobak, P. Guzdek, A. Błachowski, Ferroelectric ferromagnetic ceramic composites based on PZT with added ferrite. Int. J. Appl. Ceram. Technol. **12**, 82–89 (2015)
19. T. Kimura, Spiral magnets as magneto electrics. Annu. Rev. Mater. Res. **37**, 387–413 (2007)
20. A.V. Trukhanov, S.V. Trukhanov, V.G. Kostishin, L.V. Panina, M.M. Salem, I.S. Kazakevich, V.A. Turchenko, V.V. Kochervinskiie, D.A. Krivchenyab, Multiferroic properties and structural features of M-type al-substituted barium hexaferrites. Phys. Solid State 59(4), 737–745 (2017) (ISSN 1063-7834)
21. K. Zvezdin, A.P. Pyatakov, Phase transitions and the giant magneto electric effect in multiferroics. Phys. Usp. **47**(4), 416 (2004)
22. A.V. Trukhanov, V.O. Turchenko, I.A. Bobrikov, S.V. Trukhanov, I.S. Kazakevich, A.M. Balagurov, Crystal structure and magnetic properties of the $BaFe_{12-x}Al_xO_{19}$ ($x = 0.1$–1.2) solid solutions. J. Magn. Magn. Mater. **393**, 253–259 (2015)
23. V. Adelsköld, X-ray studies on magneto-plumbite, $PbO{\cdot}6Fe_2O_3$, and other substances resembling "beta-alumina", $Na_2O{\cdot}11A_2O_3$. Ark. Kemi Mineral. Geol. Ser. A-12 **29**, 1–9 (2003)
24. V.A. Turchenko, A.V. Trukhanov, I.A. Bobrikov, S.V. Trukhanov, A.M. Balagurov, Study of the crystalline and magnetic structures of $BaFe_{11.4}A_{l0.6}O_{19}$ in a wide temperature range. J. Surf. Investig. X-ray Synchrotron Neutron Tech. **9**(1), 17–23 (2015)
25. S.V. Trukhanov, A.V. Trukhanov, V.A. Turchenko, V.G. Kostishin, L.V. Panina, I.S. Kazakevich, A.M. Balagurov, Crystal structure and magnetic properties of the $BaFe_{12-x}In_xO_{19}$ ($x = 0.1$–1.2) solid solutions. J. Magn. Magn. Mater. **417**, 130–136 (2016)
26. A.V. Trukhanov, S.V. Trukhanov, L.V. Panina, V.G. Kostishyn, I.S. Kazakevich, An.V. Trukhanov, E.L. Trukhanova, V.O. Natarov, V.A. Turchenko, M.M. Salem, A.M. Balagurov, Evolution of structure and magnetic properties for $BaFe_{11.9}Al_{0.1}O_{19}$ hexaferrite in a wide temperature range. J. Magn. Magn. Mater. **426**, 487–496 (2017)
27. S.V. Trukhanov, A.V. Trukhanov, V.G. Kostishyn, L.V. Panina, V.A. Turchenko, I.S. Kazakevich, An.V. Trukhanova, E.L. Trukhanova, V.O. Natarov, A.M. Balagurov, Thermal evolution of exchange interactions in lightly doped barium hexaferrites. J. Magn. Magn. Mater. **426**, 554–562 (2017)
28. S.V. Trukhanov, A.V. Trukhanov, V.G. Kostishyn, L.V. Panina, V. An, V.A. Trukhanov, D.I. Turchenko, E.L. Tishkevich, V.V. Trukhanova, O.S. Oleynik, L.Yu. Yakovenko, D.A. Matzui, Vinnik, Magnetic, dielectric and microwave properties of the $BaFe_{12-x}Ga_xO_{19}$ where ($x = 0.2$–1.2) solid solutions at room temperature. J. Magn. Magn. Mater. **442**, 300–310 (2017)
29. M.H. Makled, T. Matsui, H. Tsuda, H. Mabuchi, M.K. El-Mansy, Magnetic and dynamic mechanical properties of barium ferrite-natural rubber composites. J. Mater. Process. Technol. **160**, 229–233 (2005)
30. A. Mali, A. Ataie, Structural characterization of nanocrystalline $BaFe_{12}O_{19}$ powders synthesized by sol–gel combustion route. Scr. Mater. **53**, 1065–1075 (2005)
31. I.A. Auwal, A. Baykal, S. Güner, M. Sertkol, H. Sözeri, Magneto-optical properties $BaBi_xLa_xFe_{12-2x}O_{19}$ ($0.0 \leq x \leq 0.5$) hexaferrites. J. Magn. Magn. Mater **409**, 92–98 (2016)
32. L.S.I. Liyanage, S. Kim, Y.K. Hong, J.H. Park, S.C. Erwin, S.G. Kim, Theory of magnetic enhancement in strontium hexaferrite through Zn–Sn pair substitution. J. Magn. Magn. Mater **348**, 75–81 (2013)
33. R. Nowosielski, R. Babilas, G. Dercz, L. Pająk, J. Wrona, Structure and properties of barium ferrite powders prepared by milling and annealing. Arch. Mater. Sci. Eng. **28**(12) 735–742 (2007)
34. I. Bsoul, S.H. Mahmood Jordan, Structural and magnetic properties of $BaFe_{12-x}Al_xO_{19}$ prepared by milling and calcination. J. Phys. **2**(3), 171–179 (2009)
35. A.G. Angelesa, G.M. Suareza, A. Gruskova, M. Papánova, J. Slamac, Magnetic studies of Zn–Ti-substituted barium hexaferrites prepared by mechanical milling. Mater. Lett. **59**, 26–31 (2005)
36. O. Kubo, E. Ogawa, Barium ferrite particles for high density magnetic recording. J. Magn. Magn. Mater. **134**, 376–381 (1994)
37. E.W. Gorter, Saturation magnetization and crystal chemistry of ferromagnetic oxides. Philips Res. Rep. **9**, 295–320 (1954)
38. I. Arvanitidis, Du. Siche, S. Seetharaman, A study of thermal decomposition of $BaCo_3$. Metall. Mater. Trans. B **27**(3), 409–416 (1996)
39. V. Cabuil, Phase behavior of magnetic nano particles dispersions in bulk and confined geometries. Curr. Opin. Colloid Interface Sci. **5**, 44–48 (2000)
40. S. Ounnunkad, P. Winotai, Properties of Cr-substituted M-type barium ferrites prepared by nitrate–citrate gel-auto-combustion process. J. Magn. Magn. Mater. **301**(2), 292–300 (2006)

41. S.K. Sahoo, K. Agarwal, A.K. Singh, B.G. Polke, K.C. Raha, Characterization of γ- and α-Fe_2O_3 nano powders synthesized by emulsion precipitation–calcination route and rheological behaviour of α-Fe_2O_3. Int. J. Eng. Sci. Technol. **2**(8), 118–126 (2010)
42. X. Shi, Y. Pu, D. Liu, Preparation of magnetic barium ferrite powders by microwave hydrothermal method. J. Ceram. Process. Res. **13**(Special. 2), 414–417 (2012)
43. E.K. Joongho Dho, J.Y. Lee, N.H. Park, Hur, Effects of the grain boundary on the coercivity of barium ferrite $BaFe_{12}O_{19}$. J. Magn. Magn. Mater. **285**, 164–168 (2005)
44. J. Krishna murthy, C. Mitra, S. Ram, A. Venimadhav, Temperature dependent magnetic and dielectric properties of M-type hexagonal $BaFe_{12}O_{19}$ nanoparticles. J. Alloy. Compd. **545**, 225–230 (2012)
45. Y.F. Lu, W.D. Song, Properties of $BaFe_{12}O_{19}$ films prepared by laser deposition with in situ heating and post annealing. Appl. Phys. Lett. **76**, 490 (2000). https://doi.org/10.1063/1.125797
46. L. Hongfei, W. Jianjiang, X. Baocai, L. Guanhui, L. Zhiguang, H. Yongshen, W. Guoshun, G. Haitao, Y. Liang, Single-phase $Mn_{1-x}Zn_xFe_2O_4$($x = 0.2, 0.5, 0.8$) hollow ceramic microspheres: one-step preparation and electromagnetic properties. J. Appl. Phys. **116**, 174311 (2014)
47. G. Mendoza-Suarez, J.A. Matutes-Aquino, J.I. Escalante-Garcia, H. Mancha-Molinar, D. Rios-Jara, K.K. Johal, The effect of condensation on the morphology and magnetic properties of modified barium hexaferrite ($BaFe_{12}O_{19}$). J. Magn. Magn. Mater **223**(55), 27 (2001)